A novel length back-calculation approach accounting for ontogenetic changes in the fish length – otolith size relationship during the early life of sprat (*Sprattus sprattus*)

Claudia C. Günther, Axel Temming, Hannes Baumann, Bastian Huwer, Christian Möllmann, Catriona Clemmesen, and Jens-Peter Herrmann

Abstract: An individual-based length back-calculation method was developed for juvenile Baltic sprat (*Sprattus sprattus*), accounting for ontogenetic changes in the relationship between fish length and otolith length. In sprat, metamorphosis from larvae to juveniles is characterized by the coincidence of low length growth, strong growth in body height, and maximal otolith growth. Consequently, the method identifies a point of metamorphosis for an individual as the otolith radius at maximum increment widths. By incorporating this information in our back-calculation method, estimated length growth for the early larval stage was more than 60% higher compared with the result of the biological intercept model. After minimal length growth during metamorphosis, we found the highest increase in length during the early juvenile stage. We thus located the strongest growth potential in the early juvenile stage, which is supposed to be critical in determining recruitment strength in Baltic sprat.

Résumé : Une méthode de rétrocalcul de la longueur basée sur les individus a été mise au point pour le sprat (*Sprattus sprattus*) juvénile, qui explique les modifications ontogéniques de la relation entre la longueur du poisson et la longueur des otolithes. Chez les sprats, la métamorphose des larves en juvéniles est caractérisée par la coïncidence d'un faible taux d'augmentation de la longueur, d'un taux élevé d'augmentation de la hauteur du corps et du taux de croissance maximum des otolithes. Par conséquent, la méthode définit le point de métamorphose pour un individu comme étant le rayon de l'otolithe correspondant à la largeur maximum des cernes de croissance. L'intégration de cette information à notre méthode de rétrocalcul a donné un taux d'augmentation de la longueur estimé pour le début du stade larvaire de plus de 60 % supérieur au taux prédit par le modèle d'interception biologique. Après un taux minimum d'augmentation de la longueur durant la métamorphose, la plus forte augmentation de la longueur est notée au début du stade juvénile. Ainsi, nous situons le potentiel de croissance le plus élevé au début du stade juvénile, qui est censé être un moment déterminant de l'intensité du recrutement des sprats.

[Traduit par la Rédaction]

Introduction

An important research focus in fisheries ecology is the relationship between year class strength and variable mortality rates of early life stages. Mortality during early life stages is often regarded as size-dependent and explained with the growth–mortality hypothesis (Anderson 1988), where faster growing individuals have a higher probability to survive. However, survival may either be regulated during the larval (Bailey and Houde 1989) or the juvenile life stage (Sogard 1997; Takahashi et al. 2008). To reconstruct length and growth histories of survivors and to uncover stage-specific mechanisms influencing recruitment strength, otolith microstructure analysis has been developed as a powerful tool. Generally, the otolith microstructure analysis is based on two assumptions (Campana and Jones 1992): the daily accretion of increments and a known relationship between fish length and otolith length (hereafter FL–OL relationship). Validation of daily increment formation is a mandatory procedure before applying otolith microstructure analysis to a species. How-

Received 17 November 2011. Accepted 30 April 2012. Published at www.nrcresearchpress.com/cjfas on 21 June 2012.
J2011-0474

Paper handled by Associate Editor Bronwyn Gillanders.

C.C. Günther, A. Temming, C. Möllmann, and J.-P. Herrmann. Institute for Hydrobiology and Fisheries Science, University of Hamburg, Olbersweg 24, 22767, Hamburg, Germany.
H. Baumann. School of Marine and Atmospheric Sciences, Stony Brook University, Stony Brook, NY 11794-5000, USA.
B. Huwer. DTU Aqua, National Institute of Aquatic Resources, Technical University of Denmark, Charlottenlund Slot, Jægersborg Allé 1, 2920 Charlottenlund, Denmark.
C. Clemmesen. IFM-GEOMAR, Leibniz-Institute for Marine Research at the University of Kiel, Düsternbrooker Weg 20, 24105, Kiel, Germany.

Corresponding author: Claudia C. Günther (e-mail: claudia.guenther@uni-hamburg.de).

ever, when reconstructing growth rates it is likewise important to investigate the characteristics of the FL–OL relationship to ensure that the model chosen for back-calculating length is consistent with the data (Francis 1990, 1995; Hare and Cowen 1995).

One of the first approaches to back-calculate fish length via hard parts (e.g., otoliths) is the Fraser–Lee method (Lee 1920), which uses a linear regression of the FL–OL relationship. However, it has been shown that the FL–OL relationship varies with growth rate (Mosegaard et al. 1988; Secor and Dean 1992), potentially leading to bias in back-calculated lengths derived from the Fraser–Lee method. To consider this growth effect, Campana (1990) developed the biological intercept method (hereafter BI method), which uses an empirical rather than statistical (regression-based) intercept. An extension of the BI method is the modified fry model (Vigliola et al. 2000), allowing for an allometric instead of a linear FL–OL relationship. However, the use of a back-calculation model assuming a steady FL–OL relationship is often limited to the larval stage, as the shape of the FL–OL relationship may change between life stages (e.g., Takahashi et al. 2008). For instance, in our case study on sprat, the larval stage is described by an allometric FL–OL relationship (Lee et al. 2006), whereas a linear form is assumed for the juvenile stage (Baumann et al. 2006*a*). Only a few approaches consider ontogenetic changes in the FL–OL relationship (Butler 1989; Laidig et al. 1991; Hobbs et al. 2007), allowing length reconstruction over different life stages. However, these approaches all use a population-based rather than an individual transition point between life stages. As transitions between life stages may act as critical periods with increased mortality determining the strength of a year class, there is a need to develop back-calculation methods that are applicable beyond ontogenetic changes on an individual basis (Francis 1990; Vigliola and Meekan 2009).

As it has been proven difficult to grow sprat larvae in the laboratory (Petereit et al. 2008), longitudinal records of otolith and somatic growth (e.g., Wilson et al. 2009) are not possible in Baltic sprat (*Sprattus sprattus*). In contrast with the worthwhile experimental approach to develop a back-calculation method by monitoring individual growth, we use field data of fish and otolith length and follow a regression-based approach. For this purpose, we combined data of various sampling years collected mainly during the German GLOBEC (Global Ocean Ecosystem Dynamics) project, which focused on sprat as a key species in the Baltic Sea. Sprat influences plankton communities (Kornilovs. et al. 2001) as well as top predators (Bagge et al. 1994), and its population dramatically increased after the regime shift in the late 1980s (Möllmann et al. 2009). Special attention was given to the late larval and early juvenile stage, as this stage was identified as crucial for the determination of recruitment strength (Baumann et al. 2006*b*). However, this length range (20–55 mm) cannot be captured quantitatively by commercial or scientific fishing trawls (Baumann et al. 2007). In this study, we were able to close the size class gap by sampling late larval and early juvenile stages in shallow coastal waters. The shape of the relationship between standard length and otolith radius (hereafter SL–OR relationship) of the final data set over all life stages irrevocably challenges the previously used length reconstruction method for Baltic sprat.

The objective of the study was to develop a regression-based, nonlinear back-calculation model, taking into account an allometric FL–OR relationship in the larval stage and a linear one in the juvenile stage. We hypothesize that changing body proportions during ontogeny coincide with characteristics in increment patterns on the otolith, allowing us to define an individually based point of metamorphosis. We integrated this point of metamorphosis in length back-calculation algorithms and compared the outcome with a simple nonlinear approach and a linear one, previously used for Baltic sprat.

Materials and methods

Samples

For the investigation of the relationship between SL and OR, sprat larvae (length range: ~4–20 mm SL) were sampled between 2002 and 2003 during the German GLOBEC project in the central Baltic Sea (Fig. 1; Table 1). Sampling gear was a Bongo net (diameter: 0.6 m) with a mesh size of 500 μm. Larvae were sorted out of the plankton samples directly and stored frozen. In the laboratory, SLs were recorded and sagittal otoliths prepared to measure otolith radii at the longest axis from the core to the edge. In total, data of 230 larvae from seven cruises were used. Additional to the larvae analyzed in this study, data of 58 individuals from Dänhardt et al. (2007) were added to the analysis of the SL–OR relationship (Table 1).

To detect morphometric changes in body proportions during the ontogeny of Baltic sprat, an additional subset of larvae was sampled in April 2009 in the central Baltic Sea (Table 1). Here, body heights (BHs) (at half SL) and SLs were measured to the nearest hundredth millimetre. Sampling and treatment of larvae were identical as described for the larvae used for the analysis of the SL–OR relationship (see above).

Postlarval (length range: ~20–30 mm SL) and early juvenile sprat (length range: ~30–60 mm SL) were sampled along Germany's Baltic Sea coast (Fig. 1) between July and September in 2006, 2007, and 2008 (Table 1). A 2 m × 3 m dip net with a stretched mesh size of 6 mm was used. When available, approximately 100 specimens were randomly selected, directly frozen with dry ice, and further stored at –20 °C. In the laboratory, BHs (at half SL) and SLs were measured to the nearest hundredth millimetre. Sagittal otoliths were extracted from randomly selected subsamples of individuals caught west (ST, Strande) and east (WE, Wendtorf) of the outer Kiel Fjord (Table 1). The OR was measured along the postrostral section of the otolith from the core to the edge. Thus, the following analysis of the SL–OR relationship was based on the assumption that the longest axis of the circular larval otolith will develop into the postrostral section when the otolith starts to form its characteristic shape in the postlarval stage.

Young-of-the-year (YOY) recruits (length range: ~60–90 mm SL) from the Kiel Bight were sampled in October 2007 during the annual Baltic International Acoustic Survey. Standard fishing gear of this annual survey has a stretched mesh size of 20 mm in the cod end. Random subsamples of YOY sprat were obtained from two hauls within the Kiel Bight and stored at –20 °C. In the laboratory, the same ex-

Fig. 1. Study area with sampling sites in the Baltic Sea. Black symbols represent sample sites of this study; white symbols are sample sites of other studies (see Table 1). Different shadings in the sea represent different water depths, with light grey planes corresponding to shallow areas. DE, Germany; DK, Denmark; FI, Finland; LT, Lithuania; LV, Latvia; NO, Norway; PL, Poland; RU, Russian Federation; SE, Sweden; SD, ICES subdivision.

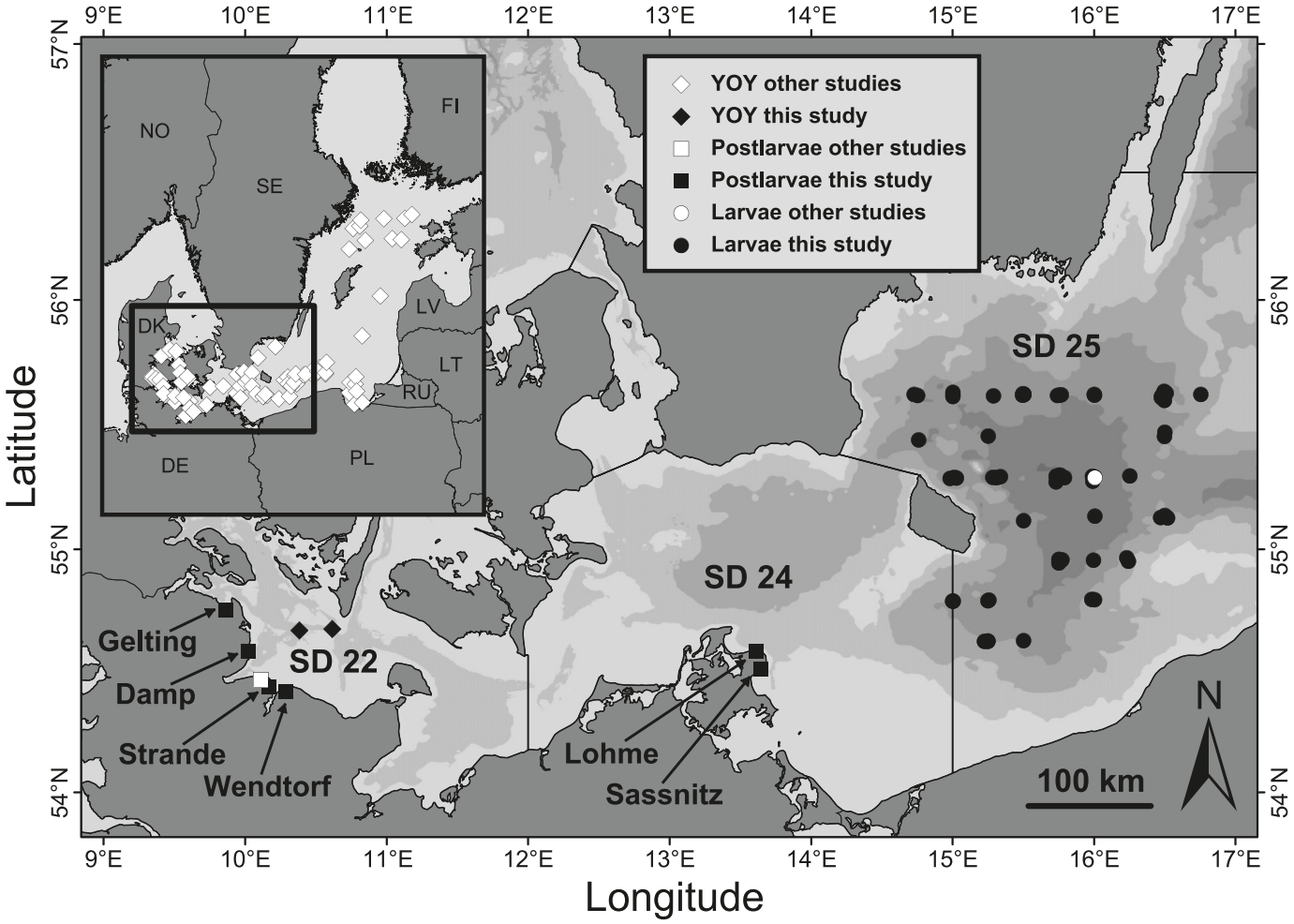

amination followed as described for postlarvae and early juveniles. YOY sprats were distinguished from 1-year-old specimens by the modes of the length–frequency distribution, with specimens smaller 90 mm SL being identified as YOY sprat, according to Baumann et al. (2006*c*).

For the investigation of the SL–OR relationship, SL and OR data of YOY sprat from previous studies were used (Table 1; Baumann et al. 2006*c*, 2008).

Otolith processing

Otolith microstructure analysis and subsequent back-calculation was performed for postlarvae and early juveniles sampled in summer 2006 and 2007 from the Kiel Fjord and for YOYs caught in October 2007 in the Kiel Bight (Table 1).

Following the extraction, sagittal otoliths were mounted on microscopic slides with a drop of thermoplastic glue (Crystalbond 509). All otoliths were ground from the convex side with a 3 μm lapping film (266x Imperial PSA 3M) until the core was reached. After reheating and turning, the other side was polished to detect the outmost increments at the edge of the postrostral section precisely. Irrespective of left or right, the otolith with the most distinct increments was chosen for analysis.

Pictures for measurement were recorded at 400× magnification with a digital camera (Leica DC300, 3132 × 2328 pixels) connected to an image analysis system (ImagePro Plus 6.0). Increments were counted and their width was measured along the axis from core to postrostrum of the otolith, beginning with the first clearly visible increment outside the core. Age estimates derived from the analysis hereafter refer to days after first increment formation.

Sufficient precision in increment counts was ascertained through intercalibration with an experienced reader, using an independent otolith subset ($n = 32$) of postlarval and juvenile sprat (20–60 mm SL). The linear regression was significant ($P < 0.001$) and explained 99% of the variance, while the slope of the regression (0.99) was not significantly different from 1 (95% confidence: 0.95–1.03). The mean coefficient of variation (Campana 2001) of all individuals was 4.4%.

Regarding otoliths used for back-calculation, increments were counted three times by the same reader, while increment widths were measured on the first and second reading. During the first reading, 222 otoliths were processed and the quality of each reading was judged according to a scale from 1 (best) to 4 (worst). Otolith readings with quality 4 ($n = 45$)

Table 1. Source of individuals used for the examination of the standard length – otolith radius (SL–OR) relationship, the body height – SL (BH–SL) relationship, and for otolith microstructure analysis and back-calculation.

							Type of analysis		
							SL–OR	BH–SL	Back-calculation
Type of sampling or gear	Source	Sampling date	Year	Location	Mean SL (mm)	Range SL (mm)	*n*	*n*	*n*
Larvae									
BIOMOC	Dänhardt et al. 2007	9–10 June	2000	SD25	13.1	9.3–21.1	58	—	—
Bongo	This study	2–30 April	2002	SD25	8.3	4.6–11.7	29	—	—
	This study	5–24 May	2002	SD25	11.0	10.1–12.2	9	—	—
	This study	11–23 June	2002	SD25	8.6	4.8–17.6	59	—	—
	This study	1–16 July	2002	SD25	12.4	8.2–26.0	36	—	—
	This study	22 July – 7 August	2002	SD25	14.6	8.6–23.0	41	—	—
	This study	15 May – 3 June	2003	SD25	11.8	10.1–14.5	23	—	—
	This study	1–19 July	2003	SD25	10.9	6.5–15.8	33	—	—
	This study	8–20 April	2009	SD25	8.0	4.3–15.0	—	192	—
Postlarvae – early juveniles									
Dip net	Baumann et al. 2007	28 August	2003	SD22-ST	35.7	28.4–45.1	51	—	—
	This study	1 August	2006	SD22-ST	29.3	23.0–36.7	30	183	23
	This study	3 August	2006	SD24-LO	29.7	22.4–48.6	—	73	—
	This study	3 August	2006	SD24-SA	35.0	22.6–41.7	—	100	—
	This study	18 August	2006	SD24-LO	43.4	36.7–55.5	—	20	—
	This study	22 August	2006	SD22-DA	50.2	44.1–58.9	—	150	—
	This study	23 August	2006	SD22-WE	57.9	46.6–65.2	29	199	26
	This study	30 August	2006	SD22-WE	60.7	42.7–69.4	16	140	15
	This study	12 September	2006	SD22-GE	43.5	33.0–59.9	—	150	—
	This study	19 July	2007	SD22-ST	41.1	35.8–52.2	36	99	26
	This study	26 July	2007	SD22-WE	51.6	43.5–56.6	27	43	21
	This study	14 August	2007	SD22-WE	25.2	21.8–29.6	83	178	31
	This study	31 July	2008	SD22-WE	23.4	19.1–25.9	27	55	—
YOY									
Trawl	Baumann et al. 2006*c*	7–29 October	2002	SD24–SD26, SD28+SD29	74.1	53–91	350	—	—
	Baumann et al. 2008	14–24 October	2002	SD22	73.8	59–86	45	—	—
	Baumann et al. 2008	5–14 October	2003	SD22	69.6	52–82	77	—	—
	Baumann et al. 2008	6–23 October	2003	SD24+SD25	77.2	67–89	69	—	—
	This study	13 October	2007	SD22	72.0	62.1–80.0	27	68	20
						Sum:	1155	1650	162

Note: YOY, young-of-the-year survivors; SD, ICES subdivision; ST, Strande; LO, Lohme; SA, Sassnitz; DA, Damp; WE, Wendtorf; GE, Gelting Mole (see Fig. 1).

were excluded from further procedure after the first reading, such that in the second and third readings, only the residual 177 otoliths were processed. Out of the first two readings where increment width was measured, the one closest to the mean of all three counts was used for further analyses, allowing a difference from the mean of maximal two increments. If the counts of the first two readings were equal, the second reading was preferred over the first one, assuming a learning curve. 74% of all otoliths exhibited a difference less than 1, while 17% showed a difference between 1 and 2. Fifteen otoliths with differences from the mean greater than 2 were excluded from the subsequent analysis. The mean coefficient of variation (Campana 2001) for the estimation of precision for the readings of the final 162 otoliths used for further analysis was 9.0%.

SL–OR relationship and nonlinear regression models

Two different approaches were used to model the overall regression of SL versus OR, which represents the basis of the length back-calculation methods explained below. Both models were developed to describe the nonlinear shape of the SL–OR relationship, which is generated by the change in body proportions during the metamorphosis from larvae to juveniles (see Results).

The first regression model describes the increase of SL with increasing OR during the larval stage by an asymptotic function followed by a linear relationship for juveniles. Both submodels, the asymptotic section and the linear section, were connected by a logistic switch-function, allowing a change between submodels and a gradual transition. SL–OR model 1 is a six-parameter function of the form

$$(1)\quad \mathrm{SL} = \left\{\mathrm{SL}_\infty \times \left[1 - \mathrm{e}^{-k\times(\mathrm{OR}+\mathrm{SL}_{\mathrm{BL}})}\right]\right\} \times \left[1 - \frac{1}{1+\mathrm{e}^{-\alpha\times(\mathrm{OR}-\mathrm{OR}_\mathrm{M})}}\right] + [a\times\mathrm{OR} + (\mathrm{SL}_\infty - a\times\mathrm{OR}_\mathrm{M})] \times \left[\frac{1}{1+\mathrm{e}^{-\alpha\times(\mathrm{OR}-\mathrm{OR}_\mathrm{M})}}\right]$$

with the parameters SL_∞, k, and SL_{BL} for the asymptotic section; a (slope) for the linear section; and α and OR_M for the logistic connection. In the section explaining length back-calculations, special attention is paid to the parameter OR_M, which describes the OR at metamorphosis when the influence of the function for the larval stage is removed by the function for the juvenile stage.

The SL–OR model 2 is structured like model 1 with the difference that the submodels for both life stages were changed. For the juvenile stage, SL–OR model 2 used a sigmoid function instead of a linear relationship, as length growth in relation to otolith growth seems to decrease for larger juveniles. To fit the sigmoid function for the juvenile stage smoothly to the data, an offset parameter (SL_{LOG}) was added to the submodel. For the larval stage, the asymptotic function of SL–OR model 1 was replaced by a power function. The technical advantage of these substitutions is that the steady increase of the power function together with the offset parameter of the sigmoid function enables the model to match the inflection point (see Results) with the parameter OR_M. To permit a smooth transition between the power and the sigmoid function while keeping the inflection point of the curve and OR_M in coincidence, α was fixed to 0.1. OR_M of the overall model was fixed to 136 μm, corresponding to the inflection point estimated by SL–OR model 1 (see Results) to permit comparability between the back-calculation approaches. Therefore, only seven of the nine parameters of SL–OR model 2 were estimated by the least square method. SL–OR model 2 was given as follows:

$$(2)\quad \mathrm{SL} = (\mathrm{SL}_{\mathrm{POW}} + b\times\mathrm{OR}^c)\times\left[1 - \frac{1}{1+\mathrm{e}^{-\alpha\times(\mathrm{OR}-\mathrm{OR}_\mathrm{M})}}\right] + \left\{\mathrm{SL}_{\mathrm{LOG}} + \mathrm{SL}_{\mathrm{MAX}}\times\left[\frac{1}{1+\mathrm{e}^{-\beta\times(\mathrm{OR}-\mathrm{OR}_\mathrm{J})}}\right]\right\} \times \left[\frac{1}{1+\mathrm{e}^{-\alpha\times(\mathrm{OR}-\mathrm{OR}_\mathrm{M})}}\right]$$

The parameters SL_{POW}, b, and c belong to the power section; SL_{LOG}, SL_{MAX}, β, and OR_J to the sigmoid section; and α and OR_M to the logistic connection.

To assure an equal influence of all life stages on the regression, a subset of 40 individuals per 10 mm length class was randomly selected to estimate the parameters of SL–OR models 1 and 2. Therefore, only 360 individuals were finally applied for the estimation using SPSS 17.0 (SPSS Inc., Chicago, Illinois). To prove if the random selection of 40 individuals per length class has an influence on the estimation, four additional data sets were created in the same way and used for the same regression. Parameters and confidence limits of the total five regression runs were compared for profound differences in each model. For the evaluation of the best regression model, Akaike's information criterion (AIC) was used.

BH–SL relationship

A modification of the Gompertz model was fitted to the relation of relative body height (as percentage of SL) and SL (n = 1650; Table 1) to detect changes in body proportions throughout the development of young sprat:

$$(3)\quad \mathrm{BH} = s + \mathrm{BH}_\infty \times \mathrm{e}^{-\mathrm{e}^{-g(\mathrm{SL}\times x_0)}}$$

where BH is the relative body height; BH_∞, g, and x_0 are the common parameters of the Gompertz model; and s is an added offset parameter. Parameters s and BH_∞ add up to the maximum in relative body height.

Length back-calculation

Three different approaches for back-calculating previous length in Baltic sprat were developed (Fig. 2; Table 2) and compared with each other as well as with the BI method (Campana 1990) with a biological intercept of 5 mm SL as in Baumann et al. (2006*a*). All length back-calculations were performed in MS Excel 2000.

The BI method is independent of the regression of SL and OR but assumes a linear relationship between SL and OR throughout the back-calculation period and considers the growth effect by generating a back-calculation line between two known fixed points (Fig. 2): the empirically estimated biological intercept and the point defined by fish length and otolith length at capture.

Our first approach is based on the regression of SL–OR model 1 and is called the nonlinear regression method (here-

Fig. 2. Schematic illustration of back-calculation approaches: (*a*) biological intercept method (Campana 1990); (*b*) nonlinear regression method; (*c*) metamorphosis method; (*d*) metamorphosis inflection point method. Black cross: length at catch of individual *j*. Grey dashed line: overall regression of the SL–OR relationship $f(\mathrm{OR_{all}})$. Black solid line: back-calculation line $f(\mathrm{OR}_j)$ of individual *j*. Black dashed line: initial back-calculation line $f(\mathrm{OR_{M}}_j)$ with OR-at-maximum increment width as $\mathrm{OR_M}$.

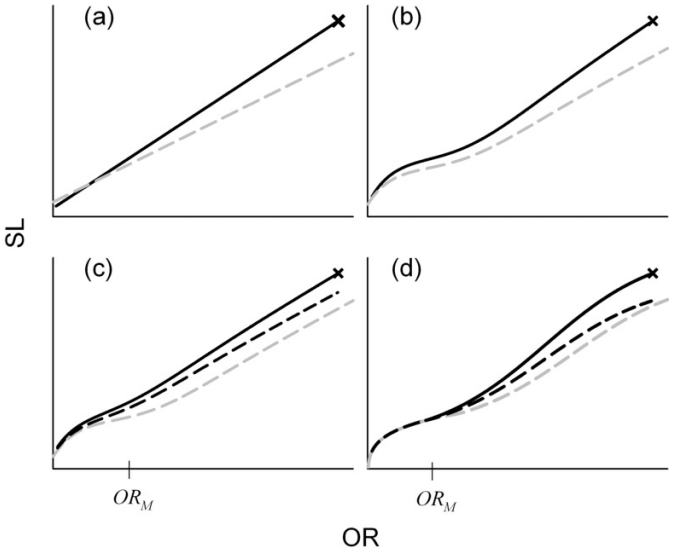

after NLR method) (Table 2). The general goal of this approach is to generate a line between two fixed points in a nonlinear way. This procedure is also known as the body-proportional hypothesis (BPH) and assumes a constant proportional deviation of an individual's fish length from the mean fish size throughout life (Francis 1990). In other words, the individual back-calculation line of the *j*th individual ($f(\mathrm{OR}_j)$) was developed by the multiplication of the overall regression $f(\mathrm{OR_{all}})$ with the ratio of the *j*th individual's SL at the time of capture (SL_{cj}) and the corresponding SL of $f(\mathrm{OR_{all}})$ at the *j*th individuals OR at time of capture ($f(\mathrm{OR_{all}}_{cj})$):

$$f(\mathrm{OR}_j) = f(\mathrm{OR_{all}}) \times \left[\frac{\mathrm{SL}_{cj}}{f(\mathrm{OR_{all}})}\right] \quad (4)$$

The only difference between the NLR method and the BPH (eq. 4) is a common *y* intercept for all individual back-calculation lines. This common starting point is generated by subtracting the regression-based *y* intercept of SL–OR model 1 from the overall SL–OR relationship before multiplying it with the individual length ratio and adding it again afterwards. Thus, the nonlinear overall regression curve of SL–OR model 1 is rotated around the *y* intercept until the curve crosses the fish length and otolith length at capture (Fig. 2). The *y* intercept equals the theoretical length when the otolith radius is zero. Therefore, resulting SL at first increment formation (comparable to the biological intercept) depends on the individual's back-calculation line and on the OR at the first increment. After generating individual back-calculation lines, the procedure of reconstructing length at earlier ages was the same for all back-calculation approaches established here. By inserting otolith radii at ages earlier than the time of capture into the individual form of the regression model, previous length of the corresponding specimen can be calculated.

In contrast with the former approach, the following two methods implement an additional fixed point into the back-calculation procedure (Fig. 2): the point of metamorphosis (see Results). As opposed to the *y* intercept (or biological intercept) and the length at capture, the point of metamorphosis is defined by an *x* value (OR) only. Furthermore, this point is not common for all individuals from the population (as it is the case with the biological intercept), but is specific for every individual, as it refers to the OR when the maximal increment widths (hereafter OR-at-maximum increment width) are established on the individual otolith. To determine the OR-at-maximum increment width, the following model was fitted to increment width versus age for every individual:

$$\mathrm{IW} = R \times \mathrm{e}^{(a_1 \times \mathrm{AGE})} \times \left[1 + \frac{1}{1 + \mathrm{e}^{-a_2 \times (\mathrm{AGE} - \mathrm{AGE_M})}}\right] \quad (5)$$

The parameters R, a_1, a_2, and $\mathrm{AGE_M}$ are estimated by the least square method. Originally created to describe a temperature optimum of a physiological rate (Temming 1995), the model is likewise able to reproduce the exponential increase of increment width in the larval stage combined with a maximum and followed by a decrease in the juvenile stage. The corresponding OR at the age when maximum increment width occurred was used as point of metamorphosis and applied in the parameter $\mathrm{OR_M}$ in the following back-calculation approaches. As we assume metamorphosis as a period in life rather than a single day, we model OR-at-maximum increment width instead of using the observed OR when the maximal increment occurred on the otolith. By doing so, we estimate a value that describes the middle of metamorphosis.

We called our second back-calculation approach metamorphosis method (hereafter M method) (Table 2), as it was the first attempt to incorporate OR-at-maximum increment width on an individual basis. The M method is based on the regression of SL–OR model 1, and individual back-calculation lines were created in two steps. In step A, OR-at-maximum increment width was derived from the individual fit of eq. 5 and was then applied in SL–OR model 1 as $\mathrm{OR_M}$ (i.e., the otolith radius when the influence of the asymptotic section is removed by the linear section). All other parameters of SL–OR model 1 were fixed as estimated by the overall regression. The resulting curve is referred to as $f(\mathrm{OR_{M}}_j)$ (Fig. 2). In step B, the individual back-calculation line ($f(\mathrm{OR}_j)$) is generated as in NLR method, by rotating $f(\mathrm{OR_{M}}_j)$ around the intercept (Fig. 2).

Our last and final approach based on the regression of SL–OR model 2 and was called the metamorphosis inflection point method (hereafter MIP method) (Table 2). As variability in the larval phase was low compared with the juvenile stage, only the right part of the back-calculation line starting at $\mathrm{OR_M}$ (instead of the intercept) was rotated in the MIP method, resulting in an almost identical line for individual larval phases. The development of individual back-calculation lines in this approach followed four steps: In step A, the OR-at-maximum increment width was used as $\mathrm{OR_M}$, as in the M method. The difference between $\mathrm{OR_M}$ of the overall regression and the OR-at-maximum increment width was added to $\mathrm{OR_J}$ in step B. Depending on the value of $\mathrm{OR_M}$, the model may exhibit an abrupt change between the power function and the sigmoid function. To smooth the

Table 2. Characteristics and differences of back-calculation approaches.

Method	Assumption for SL–OR relationship	Additional fixed point at metamorphosis	Adjustment to individual back-calculation line	Type of larval submodel	Type of juvenile submodel
Biological intercept	Linear (regression independent)	No	NA	NA	NA
Nonlinear regression	Nonlinear (regression dependent)	No	Rotation around intercept	Asymptotic	Linear
Metamorphosis	Nonlinear (regression dependent)	Yes	Rotation around intercept	Asymptotic	Linear
Metamorphosis inflection point	Nonlinear (regression dependent)	Yes	Rotation around OR_M	Power	Sigmoid

generated curve the offset parameter SL_{LOG} of the sigmoid function was corrected for the SL of the power function at OR_M in step C. In other words, the sigmoid fraction for the juvenile stage was adjusted in *y* direction to allow a smooth transition. Finally, the initial back-calculation line ($f(OR_{Mj})$) for individual *j* is rotated around OR_M to the corresponding SL–OR point at capture in step D. In doing this, the starting point for the BPH (eq. 4) and thus the multiplication of $f(OR_{Mj})$ with the ratio of SL_{cj} and the corresponding SL of $f(OR_{Mj})$ at the OR at the time of capture ($f(OR_{Mcj})$ is OR_M (Fig. 2).

To compare and demonstrate the performances of the different back-calculation approaches, data from 2006 and 2007 (Table 1) caught in the Kiel Bight were used for implementation and illustration.

Results

Ontogenetic changes in morphometry

The raw data of the SL–OR relation exhibited two conspicuous features (Figs. 3*a*, 3*b*): a distinct pattern for early life stages and an increasing variability in SL with increasing OR. Concerning the former, SL in the early larval stage was increasing rapidly with OR, while in the late larval stage, this increase was gradually reduced, resulting in a minimum of the gradient. In the subsequent juvenile phase, the slope of the raw data increased again to remain constant for most of the juvenile stage.

Both models developed here to describe the SL–OR relation (SL–OR models 1 and 2) showed an equal performance and were able to appropriately model the course of both life stages by explaining more than 97% of the overall variability in SL. The selection of a subset of data to assure an equal influence of all life stages on the regression has only a negligible effect on the parameter estimates (Table 3). Parameters of five equally performed estimation runs, basing on five randomly selected data sets, were inside the confidence limits of each other for both SL–OR models. Regarding the AIC, SL–OR model 2 performed slightly better than SL–OR model 1. Common for both models was the logistic switch-function, with the parameter OR_M describing the OR when the influence of the function for the larval stage was replaced by the function for the juvenile stage. In SL–OR model 1, where an asymptotic function for the larval stage was combined with a linear function for the juvenile phase, OR_M was estimated at 198 μm OR. However, the inflection point of SL–OR model 1, where the gradient was lowest and thus otolith growth was strongest in relation to length growth, was located at 136 μm OR (Fig. 3*a*).

In contrast, SL–OR model 2 was composed of a power function for the larval stage and a sigmoid function for the juvenile phase (Fig. 3*b*). The combination of these submodels and its offset parameters enabled the overlay of the inflection point of the curve (138 μm; Fig. 3*b*) with the parameter OR_M (136 μm).

Model 3 was used to describe the relationship between relative body height and SL and explained 96% of the variability in body height. Despite the lack of data between 15 and 20 mm SL (Fig. 3*c*), relative body height showed a distinct s-shaped form with increasing SL. The inflection point of model 3, where growth in body height was strongest in relation to SL, was estimated near to the edge of the data gap at 20.1 mm SL. When relative body height reached 20.2% at about 50 mm SL, length and height approximately grew in the same relation, indicating isometric growth in body proportions at sizes bigger than 50 mm SL.

The mean OR corresponding to maximum increment width of all individuals was calculated as 168 μm (Fig. 3*d*). For the M method and the MIP method, model 5 was fitted to individual increment width-at-age trajectories to obtain the age when maximum increment width occurred. As age and OR-at-maximum increment width were highly correlated ($p < 0.05$, $r^2 = 0.82$), the corresponding otolith radius was used as OR-at-maximum increment width and therefore as individual OR_M for length back-calculation. Model 5 explained on average 89.99% ± 0.05% of the variability in increment width. On average, modelled and observed OR-at-maximum increment width differed by 56 μm (Fig. 3*d*).

The length when all three ontogenetic changes in morphometry occurred (changing SL–OR relationship, strongest increase in the body height – SL relationship, and maximum increment width on the otolith) could be located between 20.1 mm (SL at maximal growth in height) and 24.2 mm SL (corresponding SL of mean OR-at-maximum increment width). In the following, this length is called "point of metamorphosis" from larvae to juveniles. Around this point, reduced growth in length was compensated by growth in body height coinciding with maximal growth rates as reflected in largest increments on the otolith. This observation was used as base for the M method and the MIP method by inserting the individual OR-at-maximum increment width in the back-calculation algorithm. In other words, the aim was to create a back-calculation method that could model reduced length growth rates at the point of metamorphosis on an individual level.

Length back-calculation

In contrast with the previously used linear approach

Fig. 3. Morphometric changes between the larval and the juvenile stage. (*a*) SL–OR relationship with all available data described by SL–OR model 1. The larval stage (grey plane) is separated from the juvenile stage (white plane) by the inflection point of SL–OR model 1. Lengths at the inflection point are highlighted. (*b*) SL–OR relationship with all available data described by SL–OR model 2. The larval stage (grey plane) is separated from the juvenile stage (white plane) by the inflection point of SL–OR model 2. Lengths at inflection point are highlighted. (*c*) Relationship between relative body height (BH) and SL with all available data described by model 3. The larval stage (grey plane) is separated from the juvenile stage (white plane) by the inflection point of model 3. SL at inflection point is highlighted. (*d*) Mean observed increment width (IW, dark grey crosses) and standard deviation (grey bars) versus OR. Mean observed maximum IW separates the larval (grey plane) from the juvenile stage (white plane). OR at mean observed maximum IW and OR at mean modelled maximum IW is highlighted. Mean modelled increment width versus OR is shown by the black line.

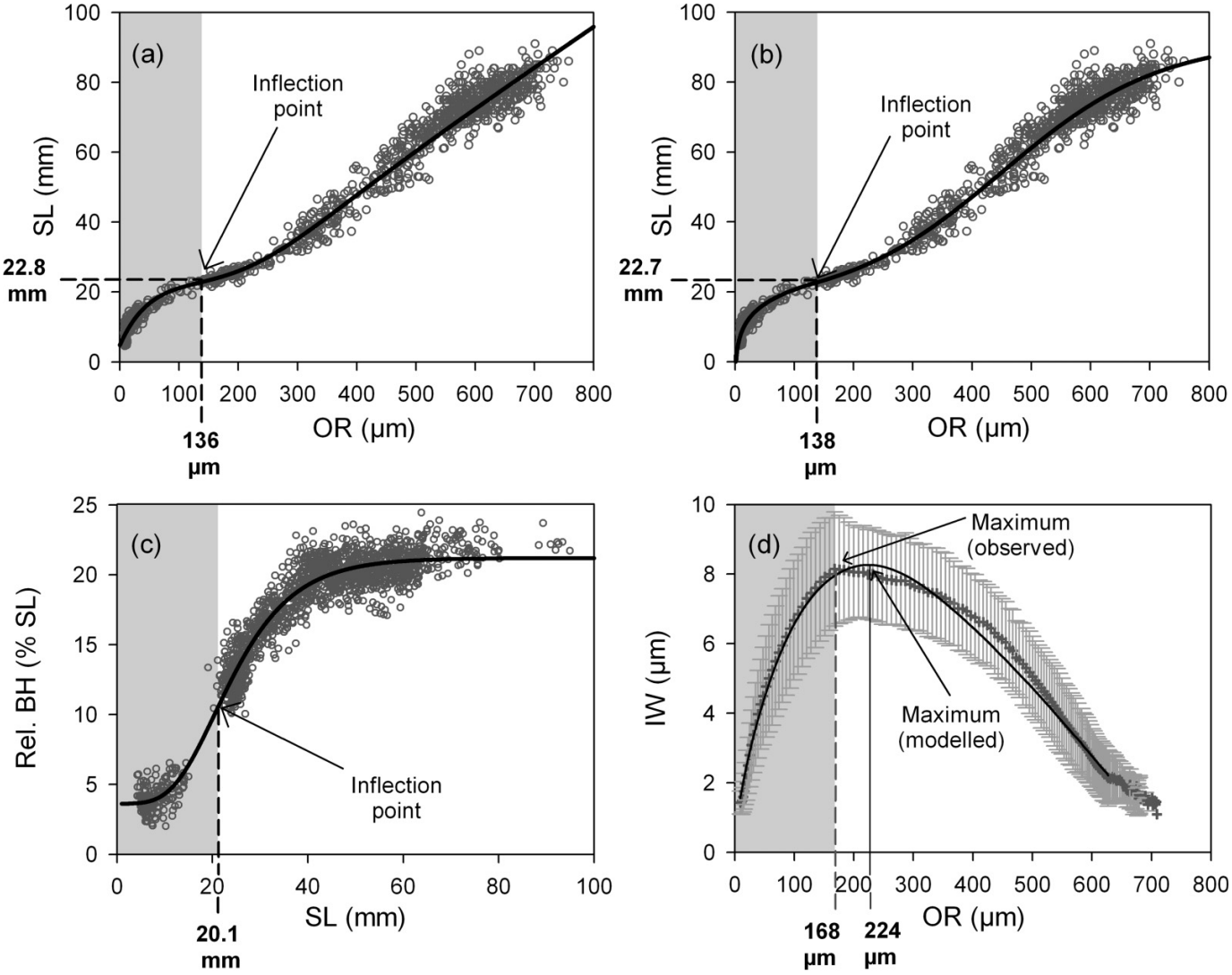

(Figs. 4*a*, 4*e*) to reconstruct length-at-age in juvenile Baltic sprat (e.g., Baumann et al. 2008), back-calculation lines of the three approaches developed here followed the nonlinear shape of the SL–OR relationship (Figs. 4*b*–4*d*, 4*f*–4*h*).

Individual back-calculation lines in the NLR method were generated assuming proportionality of the individual back-calculation line to the overall regression (Figs. 4*b*, 4*f*). This approach, which is also known as the BPH (Francis 1990), implies that a fast-growing individual will grow faster than the population mean throughout all development stages and vice versa for a slow-growing fish. In contrast, the M and MIP methods utilize the otolith radius at maximal increment width and thus define an otolith length when the larval stage ended and the juvenile stage started. This was attained by inserting the OR-at-maximum increment width as OR_M in SL–OR models 1 and 2, respectively. As the point of metamorphosis was fixed on an individual level, poor growth in early life may be compensated by accelerated growth as a juvenile. As in the NLR method, back-calculation lines in the M method were produced by rotating the curve around the intercept after inserting OR-at-maximum increment width in the regression model (Figs. 4*c*, 4*g*). In contrast, rotation of the individual back-calculation lines in the MIP method started at OR_M. This procedure generated almost one common back-calculation line in the larval stage, as the individual OR_M was the only feature influencing the course at the beginning (Figs. 4*d*, 4*h*).

As inferred by length growth rates of all back-calculation

Table 3. Parameter estimates, standard errors, and confidence limits of the first estimation run and AICs of SL–OR models 1 and 2.

(*a*) Model 1, AIC = 415.08.

		Parameter estimate					
	Run	SL_∞	SL_{BL}	k	α	OR_M	a
	1	26.084	10.746	0.019	0.012	197.967	0.116
	2	25.126	10.851	0.020	0.012	185.771	0.116
	3	26.015	9.729	0.021	0.012	200.931	0.119
	4	25.802	12.383	0.019	0.013	194.477	0.118
	5	26.347	14.824	0.016	0.013	198.878	0.118
Standard error	1	2.203	6.827	0.008	0.005	29.972	0.003
95% Confidence limits	1	21.752–30.416	–2.680–24.172	0.004–0.035	0.003–0.022	139.020–256.914	0.111–0.121

(*b*) Model 2, AIC = 403.74.

		Parameter estimate					
	Run	SL_{POW}	b	c	β	OR_J	SL_{MAX}
	1	–38.261	36.398	0.104	0.007	449.565	76.415
	2	–32.116	30.589	0.118	0.007	454.926	78.338
	3	–22.241	21.550	0.148	0.008	448.988	77.369
	4	–44.961	43.097	0.089	0.007	453.275	78.375
	5	–88.793	85.481	0.054	0.008	449.065	77.489
Standard error	1	131.048	125.074	0.265	0.000	7.775	1.736
95% Confidence limits	1	–295.996–219.474	–209.587–282.384	–0.418–0.627	0.007–0.008	434.274–464.857	73.001–79.829

Note: Parameters of the 2–5 estimation run are listed.

methods, specimens caught in 2006 grew considerably faster than those of 2007 (Figs. 5*a*, 5*b*). Maximum growth rate of the linear back-calculation method was 25% lower in 2007 than in 2006. All nonlinear back-calculation methods generate bimodal growth rate patterns with high growth in the larval and maximum growth rates in the early juvenile phase, separated by a growth rate minimum around metamorphosis. The BI method reproduced highest length growth rates when widest increments were deposited on the otolith. The differences in length growth rates between the MIP method and the BI method revealed that higher length growth during the larval and the juvenile stage is estimated by the new method, whereas length growth rates at metamorphosis are reduced (Figs. 5*c*–5*f*). Mean back-calculated length at metamorphosis (OR_M) using the MIP method was 25.2 ± 1.0 mm SL in 2006 and 24.7 ± 1.4 mm SL in 2007.

During the larval stage, mean length growth estimated by the MIP method was more than 0.3 mm·day^{-1} higher as estimated by the BI method (Figs. 5*c*, 5*d*), corresponding to a 61% and 65% increase in 2006 and 2007, respectively. In contrast, the linear BI method estimated 48% higher length growth rates during metamorphosis in both years. In the early juvenile stage, the MIP method estimated again higher values than the BI method, according to 35% and 5% in 2006 and 2007 in an age range of 60–70 days, respectively.

Nonlinear back-calculation approaches differed mainly in the location of length growth minima (Fig. 6). In the NLR method, all individual length growth minima were located near the OR where the regression of SL–OR model 1 exhibited its inflection point. In the M method, the individual OR-at-maximum increment width (Figs. 6*a*, 6*b*) influenced the back-calculation line, leading to a different location of growth minima for each individual (Figs. 6*c*–6*f*). The larger the otolith was at the point of metamorphosis, the larger the discrepancy was between the NLR method and the M method. The MIP method displays peak larval growth for the youngest larval stages, while in the NLR and the M methods, this initial peak is weaker and a second pronounced peak appeared in the middle of the larval phase. In total, length growth rates of the MIP method during the larval stage were lower than those calculated by the NLR method and the M method, but mean length growth rates at metamorphosis were slightly higher (Figs. 5*a*, 5*b*). The strongest growth in length was estimated in the juvenile stage using the MIP method. Finally, length growth minima of the MIP method were located nearest to the otolith radii where maximal increment widths occur on the otoliths (Figs. 6*a*–6*f*).

Discussion

Point of metamorphosis

The point of metamorphosis between the larval and the juvenile stages was based on three morphometric features observed in a narrow length range (20.1–24.2 mm SL): (*i*) a minimum SL–OR ratio, (*ii*) maximal growth in body height, and (*iii*) peak increment width on the otolith. Feature (*i*) was derived from a data set of field-caught individuals from various years, diverse sampling sites, and different seasons and sampling methods. The detection of a consistent pattern in the SL–OR relationship of such a heterogeneous data set supports the interpretation of a true ontogenetic change. A comprehensive data set increases the likelihood of covering the whole range of growth rates occurring in nature. On the other hand, as the SL–OR relationship is known to vary with growth rate (e.g., Secor and Dean 1992), differences in the origin of individuals may be a source of uncertainty. The combined data from larvae and surviving juveniles are potentially influenced by nonrandom mortality, so that the shape of the SL–OR relationship for average larvae and for surviving juveniles may differ. However, in this case we would ex-

Fig. 4. Individual back-calculation lines (dark grey) of the different back-calculation methods generated for a subsample (black-bordered grey dots) of postlarval – early juvenile sprat caught in summer 2006 (left side) and summer and autumn 2007 (right side). (*a* and *e*) BI method; (*b* and *f*) NLR method; (*c* and *g*) M method; (*d* and *h*) MIP method. Light grey dots represent all available data.

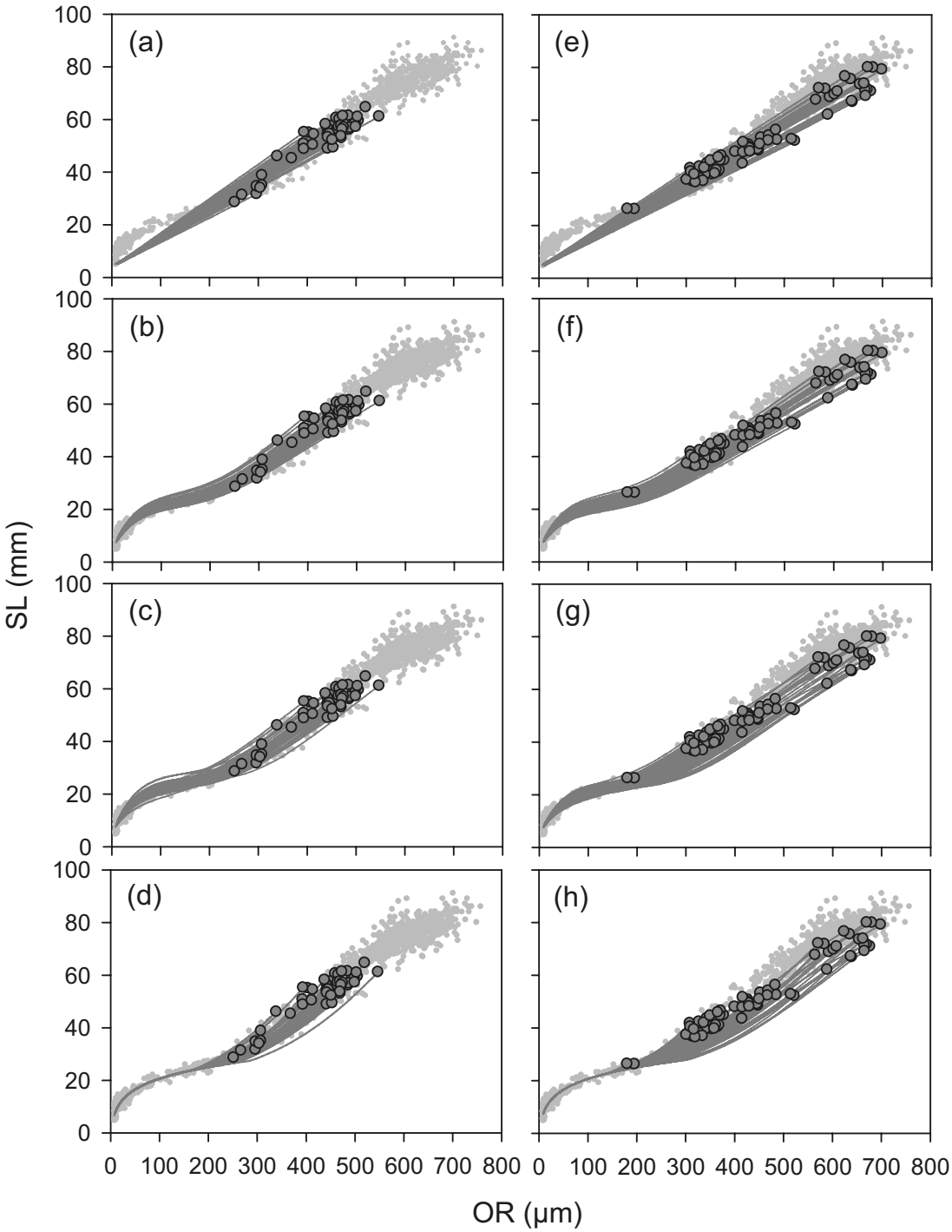

pect a larger variability in the SL–OR relationship of the smallest individuals, which is not supported by our data.

The coincidence of reduced length growth and maximal daily accretion on the otolith can be explained by accelerated growth in body height (feature (*ii*)). During metamorphosis, the shape of young sprat alters from an elongate, slender larva to a spindle-shaped juvenile body form. The change in body form comes along with an exponent of about 5 in the length–mass relationship at metamorphosis (Peck et al. 2005). Corresponding to nearly isometric growth (an exponent of 3) found for sprat beyond an SL of 44 mm described by Peck et al. (2005), we observed a constant ratio of body dimensions above an SL of 50 mm. As the otolith is assumed to record somatic growth rather than length growth, a "decoupling" in growth of fish length and otolith length would be a consequence for sprat smaller than 50 mm SL.

The third feature characterizing the point of metamorpho-

Fig. 5. Illustration of the different back-calculation methods for the mean growth of sprat caught in 2006 (left side) and 2007 (right side). (*a* and *b*) Mean back-calculated length growth rates (LGR) versus OR; (*c* and *d*) Differences between LGR calculated by the MIP method and BI method for 10-day age intervals; (*e* and *f*) Mean SL versus age.

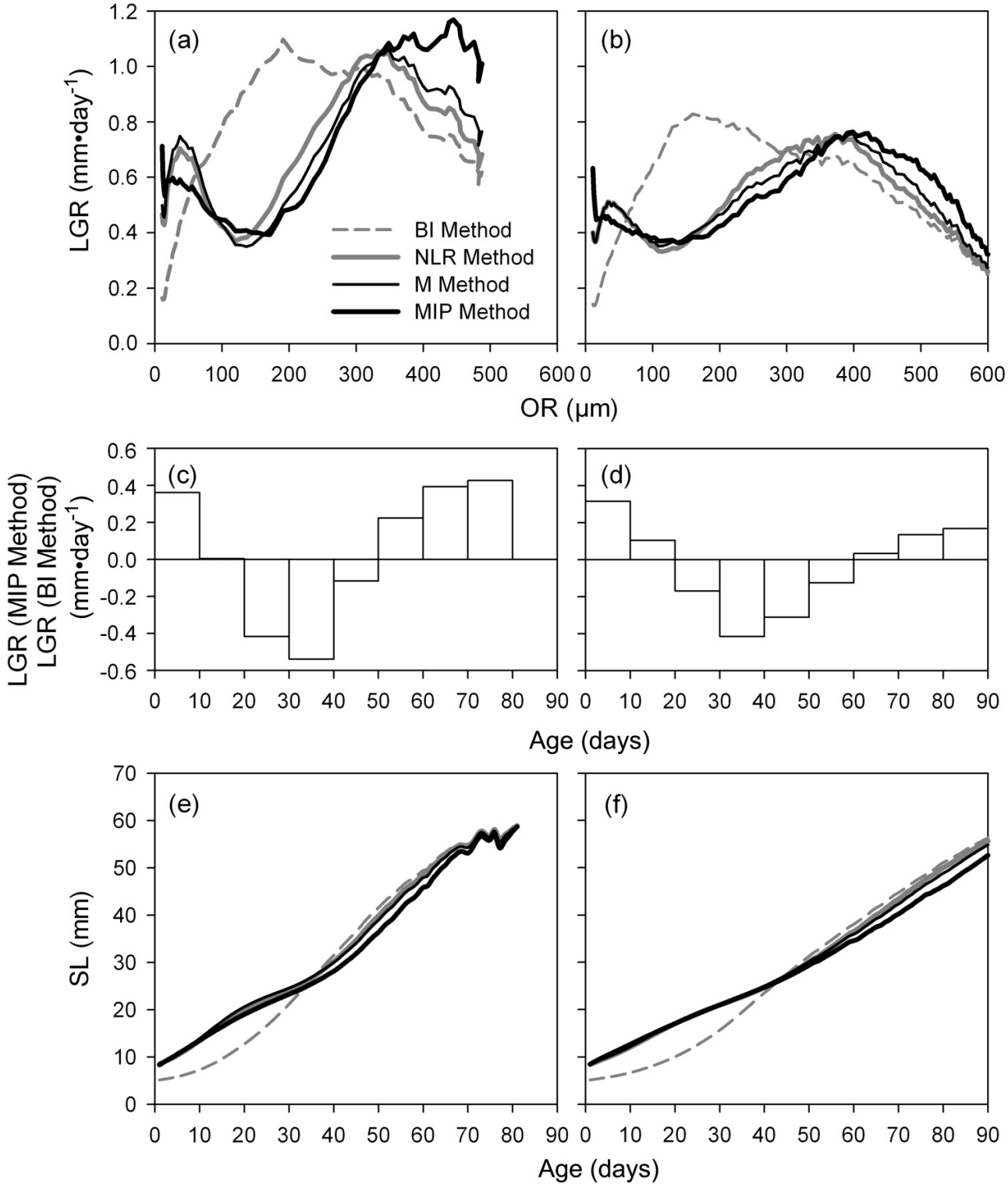

sis is the otolith increment pattern of sprat. The average OR-at-maximum increment width approximately coincides with the otolith radius where the SL–OR models have its inflection point. Strongest otolith growth during ontogeny at the same timing as lowest length growth can be explained by maximal growth in body height or mass (see above), respectively. Therefore, all three morphometric changes are linked to the same process.

Comparison of the different versions for back-calculation

Individual back-calculation lines in the NLR method were generated by two fixed points: the intercept, which is com-

Fig. 6. Illustration of the different back-calculation methods for a faster growing 50-day-old sprat from 2006 (left side) and a slower growing 98-day-old sprat from 2007 (right side). (*a* and *b*) Connected dots show observed increment width (IW) versus OR. Dashed line indicates IW versus OR as described by model 5. (*c* and *d*) Individual back-calculation lines of SL versus OR. The thin solid line represents SL–OR model 1; the thin dotted line indicates the SL–OR model 2. (*e* and *f*) Length growth rate (LGR) versus OR. The grey plane indicates the larval stage defined by the modelled OR-at-maximum increment width (dashed line in panels (*a*) and (*b*)).

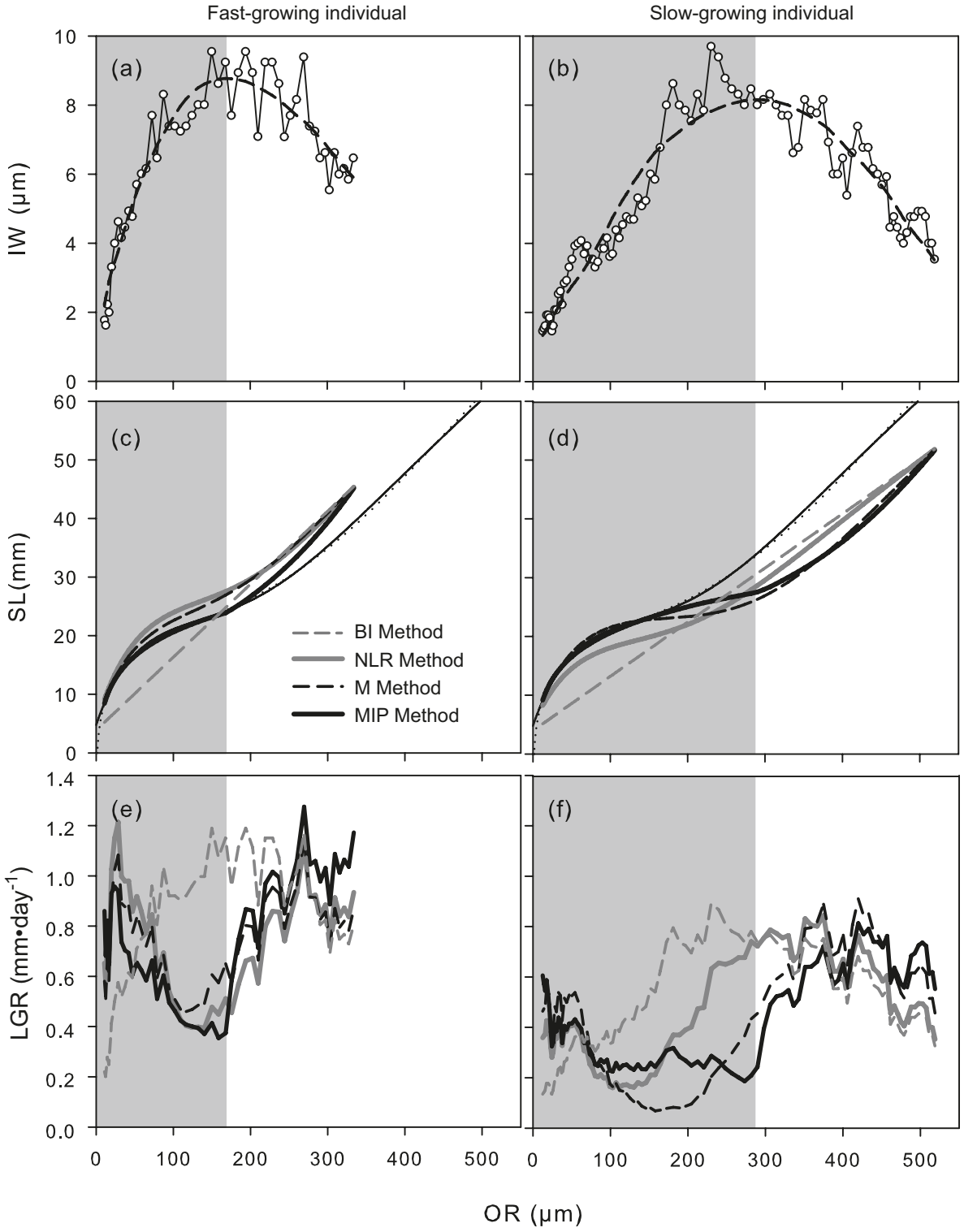

mon for all individuals, and the individual length at catch. A similar nonlinear approach was already used by Laidig et al. (1991), who modelled the SL–OR relationship by a segmented regression. The disadvantage of the NLR method is that length at metamorphosis is implicitly dependent on the length at catch.

The M method is the first attempt to consider the point of metamorphosis by the application of an individual-based OR-

at-maximum increment width. In the M method, the inflection point of an individual back-calculation line is deduced from the increment pattern of this individual. By modelling the OR-at-maximum increment width, we also determined age at metamorphosis. However, fish length at metamorphosis is defined by the overall SL–OR model 1 and is therefore almost the same for all individuals. As length at metamorphosis is fixed, but age is individually defined, the model is able to prolong the duration of the larval stage while shortening the juvenile stage and vice versa. A prolonged larval stage is associated with slow growth rates, while high growth rates occur after metamorphosis in a short juvenile stage.

However, the M method still exhibits three disadvantages. First, it is not able to implement the coincidence of maximal increment growth and minimal length growth on an individual level. Secondly, estimated length growth rates during metamorphosis of slow-growing fish may be negative. If an individual has a large OR at metamorphosis, the initial SL–OR back-calculation line may produce zero growth in length during metamorphosis. In the following step of the back-calculation algorithm, the initial SL–OR line is rotated around the *y* intercept. If an individual's length at catch has a lower SL–OR ratio than the corresponding length of the initial SL–OR line, the final back-calculation line will have a negative gradient. Finally, individual back-calculation lines of the M method can deviate substantially from the raw data observed in the larval stage, although the variability of the data in early life stages is low.

Our favoured back-calculation approach is the MIP method, which was developed to specifically address the problems of the M method. The MIP method is based on SL–OR model 2, which is able to generate individual lines, where minimal length growth rates are generated when maximum increment widths occur on the otolith. Mean back-calculated length at metamorphosis using the MIP method was slightly larger than the length range defined by a minimum SL–OR ratio, maximal growth in body height, and peak increment width on the otolith. However, the otolith-independent measure of metamorphosis is the inflection point of the relation between body height and SL. In contrast with the inflection point of model 3 at 20.1 mm SL, the raw data indicate strongest growth in body height at about 25 mm SL, which coincides with the mean back-calculated length at metamorphosis using the MIP method. Therefore, the MIP method can reproduce length growth rates considering the individual point of metamorphosis. Additionally, negative growth rates and the deviation of single back-calculation lines from the raw data in the larval stage are avoided by rotating the back-calculation line around the point of metamorphosis, instead of rotating it around the population intercept. The MIP method is quite flexible and able to reproduce length growth of individuals that are either fast-growing as larvae and slow-growing as juveniles or slow-growing as larvae and fast-growing as juveniles.

Traits of new and existing back-calculation models

Various back-calculation models have been developed concentrating on different factors influencing the relationship of somatic and otolith growth. In general, factors that control the SL–OR relationship can be grouped into two main categories: external and internal (Francis 1990; Vigliola and Meekan 2009). External factors comprise environmental conditions like temperature and food availability, whereas internal factors are related to ontogeny.

So far, particular attention has been paid to the external factors (Mosegaard et al. 1988; Secor and Dean 1992; Sirois et al. 1998), generally termed as growth effect. The growth effect describes the phenomenon that a slow-growing individual has a larger otolith than a fast-growing one of the same fish size. In the NLR and M methods, the growth effect is considered in a simple way by fixing the starting point of the back-calculation lines while constraining single lines through individual's length at catch. In our approaches, we used the regression based *y* intercept of SL–OR model 1, as Campana (1990) pointed out, that a regression-based intercept may account for the growth effect in the same way as a biological intercept if sufficient observations near the origin exist. As a comprehensive data set is required anyway when applying regression-based back-calculation models, we did not include a biological intercept in our nonlinear models. Regarding the MIP method, all individual back-calculation lines follow the overall regression of the SL–OR model 2 in the early larval stage. As a consequence, the MIP method largely neglects the growth effect during the early larval stage. Individual back-calculation lines start to deviate from each other near the point of metamorphosis. Therefore, in the juvenile stage the growth effect is considered, as back-calculation lines were rotated around the individual-based point of metamorphosis independent of the population-based regression. Thereby, the point of metamorphosis itself implements the growth effect, as individuals that were slow-growing during the larval stage have larger otoliths at metamorphosis than fast-growing ones.

Only few studies have investigated the role of internal, ontogenetic effects acting independently of growth influences and age influences on the SL–OR relationship. A modified version of the stage-specific BI model (Campana 1990), where each life stage has its own biological intercept, was implemented by Hobbs et al. (2007) to back-calculate length across a stage-specific transition of the SL–OR relationship in delta smelt larvae (*Hypomesus transpacificus*). In doing this, the authors used two biological intercepts, one for the early and the other one for the late larvae stage. Fish length at the second biological intercept was set to a fixed, population-based value. The aim of our approach was to implement the individual variation at the transition point. We observed only little variation in fish size at the point of metamorphosis in contrast with a broad range of otolith sizes. Therefore, our final approach, the MIP method, accounts for individual variation by introducing otolith size at metamorphosis in the back-calculation algorithm. Furthermore, the individual point of metamorphosis in the MIP method allows the reproduction of different growth histories per life stage. For instance, one individual may be a slow-growing larva that experienced favourable conditions as a juvenile, accelerating its growth rate, while another individual grows fast in the larval stage but experiences poor conditions as a juvenile, decelerating its growth rate. Both individuals may have the same age, fish length, and otolith radius at the end of the juvenile stage. Using a method with a fixed transition point between both life stages, like the stage-specific BI method or the NLR method, both individual growth histories would be described with exactly the same back-calculation line.

Length growth during the larval and juvenile stage of Baltic sprat

YOY Baltic sprat caught in autumn are predominantly composed of individuals born late in the season (Baumann et al. 2008). The strength of the year class is assumed to be determined during the late larval and early juvenile stage (Köster et al. 2003). Interestingly, our nonlinear back-calculation methods located the strongest potential for length growth likewise in the early juvenile stage.

Beside a high and nonrandom mortality, strong length growth potential is a required condition for the occurrence of size-selective mortality (Sogard 1997). The survival of faster growing juveniles and the subsequent disadvantage of slow-growing individuals may be the consequence of two mortality sources: starvation and predation (Heath 1992). Sogard (1997) highlighted the association of size-selective mortality caused by starvation with the overwinter mortality in temperate fish species. However, Köster et al. (2003) examined the relationship between successive life stages and found the abundance of 0-group Baltic sprat in autumn as a good predictor of the abundance of 1-year-old recruits. This suggests that overwinter mortality cannot explain strong interannual recruitment variability in Baltic sprat.

Concerning predation, bigger size may benefit the survival in the presence of predators (e.g., Anderson 1988). Juvenile sprat are predominantly found in nearshore habitats (Parmanne et al. 1994; Arrhenius 1998). Studies discussing possible predators of juvenile sprat in these nearshore nursery areas are rare. Generally, one of the most important predators of adult sprat in the Baltic Sea is Atlantic cod (*Gadus morhua*) (Bagge et al. 1994). Although, it is known that predation by cod can influence the size of the sprat stock (Rudstam et al. 1994), there is no evidence that small differences in prey size have an effect on total mortality. However, during our sampling period in shallow waters of the Kiel Bight, we observed young garfish (*Belone belone*) frequently hunting on schools of early juvenile sprat. As sprat became larger (~50 mm SL) at the end of the season, predation could no longer be observed, whereas juvenile sprat seemed to be highly mobile. Being larger may improve swimming and escaping abilities and therefore benefit the survival. Further research on nursery areas is needed to confirm these observations and to identify predators, their size preferences, and their role in influencing the year class strength of Baltic sprat.

Back-calculating length beyond ontogenetic transitions

By incorporating the point of metamorphosis in a nonlinear back-calculation model, the MIP method produces mean length growth rates during the early larval stage that were more than 60% higher than estimates of the previously used BI method. This bias in growth estimates can cause profound misinterpretations of ecological processes. For instance, an underestimation of length growth during the larval stage would suggest high mortality rates induced by predators, as these small larvae would remain for a prolonged period in the size spectrum of many predators (Ware 1975; Anderson 1988). In drift simulations, such an underestimation of length growth rates may lead to a biased estimation of the planktonic stage duration. Because the onset of active swimming starts earlier if larvae grow faster, the predicted locations of post-larvae habitats may be likewise biased (Baumann et al. 2006*b*).

Beside considerable differences in length growth rates during the larval stage, profound changes between the MIP and BI methods were found at metamorphosis from larvae to juveniles. Using the MIP method, low length growth is recorded during metamorphosis followed by maximal length growth rates during the juvenile stage. In contrast, the BI method generates a maximum growth rate in length during metamorphosis and a decrease afterwards. Laboratory studies on investigating growth during the first months of life that encompass the larval as well as the juvenile stage are rare. Nakamura et al. (1991) conducted a rearing experiment from hatching to the juvenile stage with Japanese sardine (*Sardinops melanostictus*), a species similar to Baltic sprat, exhibiting a transition from an elongate larval form to a spindle-shaped juvenile body form. Results of this study located low growth rates in length at the transition between both life stages, whereas highest growth rates in length occur during the juvenile stage.

In general, transitions between ontogenetic stages are often accompanied by changes in behaviour. In the case of clupeids, metamorphosis comes along with a niche shift from transparent larvae, which are passive, drifting planktonic particles, to pigmented and scaled juveniles, which are active swimmers. Such a change between life stages may cause short-term stagnation of length growth, because other adaptions to new lifestyle requirements (e.g., spindle shape, scales) were favoured over size increase. Beside clupeids, time-varying reduced growth during ontogeny can also be observed at the settlement of reef fishes (Wilson and McCormick 1997) and metamorphosis of flatfishes (e.g., Joh et al. 2011). A reduction in length growth that is accompanied with a change in the relationship of fish and otolith length leads to complications in back-calculations of length like in Baltic sprat. Just as metamorphosis in sprat, settlement of reef fishes and metamorphosis of flatfishes are critical events influencing survival and subsequent recruitment (e.g., Fukuhara 1988; Doherty et al. 2004), which makes growth reconstruction across transition points desirable for fishery ecologists. As increment pattern and morphometrics of growth differ per species and ecological niche shift, our MIP method has to be validated and adjusted for each case and species. Beside the reconstruction of length growth in sprat, the MIP method may facilitate length back-calculation over life stage transitions like settlement of reef fishes or metamorphosis in flatfishes.

Sampling postlarvae and juvenile sprat in shallow waters of the Baltic Sea enabled us to close the size class gap between the larvae and the juvenile life stages and to develop a new nonlinear back-calculation method. In contrast with the previously used BI method, the MIP method uses an individual specific point of metamorphosis and treats the allometric growth in the larval stage separately from the nearly isometric growth of the juvenile stage. Growth rates generated by the MIP method are higher during the early larval and juvenile stage than those estimated with the BI method. This result suggests that a shift in attention towards the early juvenile phase may be needed for a better understanding of processes influencing year class strength. The approach may be applicable to other species, where similar growth charac-

teristics occur during early life history. However, to apply this approach, samples of all early life stages prior to the stage of interest are needed.

Acknowledgements

We are grateful to all who were of great help during the field sampling in summer 2006 and 2007. Additionally, Andreas Dänhardt is thanked for providing his raw data. This study was funded by the Cluster of Excellence "Integrated Climate System Analysis and Prediction" (CliSAP) of the University of Hamburg. Finally, we thank the Associate Editor and the two anonymous reviewers for their valuable suggestions.

References

Anderson, J.T. 1988. A review of size dependent survival during pre-recruit stages of fishes in relation to recruiment. J. Northwest Atl. Fish. Sci. **8**: 55–66.

Arrhenius, F. 1998. Food intake and seasonal changes in energy content of young Baltic Sea sprat (*Sprattus sprattus* L.). ICES J. Mar. Sci. **55**(2): 319–324. doi:10.1006/jmsc.1997.0341.

Bagge, O., Thurow, F., Steffensen, E., and Bray, J. 1994. The Baltic cod. Dana, **10**: 1–28.

Bailey, K.M., and Houde, E.D. 1989. Predation on eggs and larvae of marine fishes and the recruitment problem. ICES J. Mar. Sci. **25**: 1–83.

Baumann, H., Hinrichsen, H.-H., Voss, R., Stepputtis, D., Grygiel, W., Clausen, L.W., and Temming, A. 2006*a*. Linking growth to environmental histories in central Baltic young-of-the-year sprat, *Sprattus sprattus*: an approach based on otolith microstructure analysis and hydrodynamic modelling. Fish. Oceanogr. **15**(6): 465–476. doi:10.1111/j.1365-2419.2005.00395.x.

Baumann, H., Hinrichsen, H.H., Möllmann, C., Köster, F.W., Malzahn, A.M., and Temming, A. 2006*b*. Recruitment variability in Baltic Sea sprat (*Sprattus sprattus*) is tightly coupled to temperature and transport patterns affecting the larval and early juvenile stages. Can. J. Fish. Aquat. Sci. **63**(10): 2191–2201. doi:10.1139/f06-112.

Baumann, H., Gröhsler, T., Kornilovs, G., Makarchouk, A., Feldmann, V., and Temming, A. 2006*c*. Temperature-induced regional and temporal growth differences in Baltic young-of-the-year sprat *Sprattus sprattus*. Mar. Ecol. Prog. Ser. **317**: 225–236. doi:10.3354/meps317225.

Baumann, H., Peck, M.A., Götze, H.E., and Temming, A. 2007. Starving early juvenile sprat *Sprattus sprattus* (L.) in western Baltic coastal waters: evidence from combined field and laboratory observations in August and September 2003. J. Fish Biol. **70**(3): 853–866. doi:10.1111/j.1095-8649.2007.01346.x.

Baumann, H., Voss, R., Hinrichsen, H.-H., Mohrholz, V., Schmidt, J.O., and Temming, A. 2008. Investigating the selective survival of summer- over spring-born sprat, *Sprattus sprattus*, in the Baltic Sea. Fish. Res. **91**(1): 1–14. doi:10.1016/j.fishres.2007.11.004.

Butler, J.L. 1989. Growth during the larval and juvenile stages of the northern anchovy, *Engraulis mordax*, in the California current during 1980–84. Fish Bull. **87**: 645–652.

Campana, S.E. 1990. How reliable are growth back-calculations based on otoliths? Can. J. Fish. Aquat. Sci. **47**(11): 2219–2227. doi:10.1139/f90-246.

Campana, S.E. 2001. Accuracy, precision and quality control in age determination, including a review of the use and abuse of age validation methods. J. Fish Biol. **59**(2): 197–242. doi:10.1111/j.1095-8649.2001.tb00127.x.

Campana, S.E., and Jones, C.M. 1992. Analysis of otolith microstructure data. *In* Otolith microstructure examination and analysis. *Edited by* D.K. Stevenson and S.E. Campana. Can. Spec. Publ. Fish. Aquat. Sci. 117. pp. 73–100.

Dänhardt, A., Peck, M.A., Clemmesen, C., and Temming, A. 2007. Depth-dependent nutritional condition of sprat *Sprattus sprattus* larvae in the central Bornholm Basin, Baltic Sea. Mar. Ecol. Prog. Ser. **341**: 217–228. doi:10.3354/meps341217.

Doherty, P.J., Dufour, V., Galzin, R., Hixon, M.A., Meekan, M.G., and Planes, S. 2004. High mortality during settlement is a population bottleneck for a tropical surgeonfish. Ecology, **85**(9): 2422–2428. doi:10.1890/04-0366.

Francis, R.I.C.C. 1990. Back-calculation of fish length — a critical review. J. Fish Biol. **36**(6): 883–902. doi:10.1111/j.1095-8649.1990.tb05636.x.

Francis, R.I.C.C. 1995. The analysis of otolith data — a mathematician's perspective (What, precisely, is your model?). *In* Recent developments in fish and otolith research. *Edited by* D.H. Secor, J.M. Dean, and S.E. Campana. University of South Carolina Press, Columbia, South Carolina. pp. 81–95.

Fukuhara, O. 1988. Morphological and functional-development of larval and juvenile *Limanda yokohamae* (Pisces, Pleuronectidae) reared in the laboratory. Mar. Biol. (Berl.), **99**(2): 271–281. doi:10.1007/BF00391990.

Hare, J.A., and Cowen, R.K. 1995. Effect of age, growth rate, and ontogeny on the otolith size – fish size relationship in bluefish, *Pomatomus saltatrix*, and the implications for back-calculation of size in fish early life history stages. Can. J. Fish. Aquat. Sci. **52**(9): 1909–1922. doi:10.1139/f95-783.

Heath, M.R. 1992. Field investigations of the early-life stages of marine fish. ICES J. Mar. Sci. **28**: 1–174.

Hobbs, J.A., Bennett, W.A., Burton, J.E., and Baskerville-Bridges, B. 2007. Modification of the biological intercept model to account for ontogenetic effects in laboratory-reared delta smelt (*Hypomesus transpacificus*). Fish Bull. **105**: 20–38.

Joh, M., Matsuda, T., Satoh, N., Tanaka, N., and Ueda, Y. 2011. Otolith microstructure of brown sole *Pseudopleuronectes herzensteini*: validation of daily ring formation and the occurrence of microstructure denoting metamorphosis. Fish. Sci. **77**(5): 773–783. doi:10.1007/s12562-011-0382-3.

Kornilovs, G., Sidrevics, L., and Dippner, J.W. 2001. Fish and zooplankton interaction in the Central Baltic Sea. ICES J. Mar. Sci. **58**(3): 579–588. doi:10.1006/jmsc.2001.1062.

Köster, F.W., Hinrichsen, H.H., Schnack, D., St John, M.A., Mackenzie, B.R., Tomkiewicz, J., Möllmann, C., Kraus, G., Plikshs, M., Makarchouk, A., and Aro, E. 2003. Recruitment of Baltic cod and sprat stocks: identification of critical life stages and incorporation of environmental variability into stock–recruitment relationships. Sci. Mar. **67**: 129–154.

Laidig, T.E., Ralston, S., and Bence, J.R. 1991. Dynamics of growth in the early life history of shortbelly rockfish *Sebastes jordani*. Fish Bull. **89**: 611–621.

Lee, R.M. 1920. A review of the methods of age and growth determination in fishes by means of scales. Fish. Investig. Lond. Ser. 2, **4**(2): 1–32.

Lee, O., Danilowicz, B.S., and Dickey-Collas, M. 2006. Temporal and spatial variability in growth and condition of dab (*Limanda limanda*) and sprat (*Sprattus sprattus*) larvae in the Irish Sea. Fish. Oceanogr. **15**(6): 490–507. doi:10.1111/j.1365-2419.2006.00406.x.

Möllmann, C., Diekmann, R., Müller-Karulis, B., Kornilovs, G., Plikshs, M., and Axe, P. 2009. Reorganization of a large marine ecosystem due to atmospheric and anthropogenic pressure: a discontinuous regime shift in the Central Baltic Sea. Glob. Change Biol. **15**(6): 1377–1393. doi:10.1111/j.1365-2486.2008.01814.x.

Mosegaard, H., Svedang, H., and Taberman, K. 1988. Uncoupling of somatic and otolith growth-rates in arctic char (*Salvelinus alpinus*)

as an effect of differences in temperature response. Can. J. Fish. Aquat. Sci. **45**(9): 1514–1524. doi:10.1139/f88-180.

Nakamura, M., Takii, K., Takaoka, O., Furuta, S., and Kumai, H. 1991. Rearing of japanese sardine from hatching through juveniles. Nippon Suisan Gakkai Shi, **57**(2): 345.

Parmanne, R., Rechlin, O., and Sjöstrand, B. 1994. Status and future of herring and sprat stocks in the Baltic Sea. Dana, **10**: 29–59.

Peck, W.A., Clemmesen, C., and Herrmann, J.P. 2005. Ontogenic changes in the allometric scaling of the mass and length relationship in *Sprattus sprattus*. J. Fish Biol. **66**(3): 882–887. doi:10.1111/j.0022-1112.2005.00651.x.

Petereit, C., Haslob, H., Kraus, G., and Clemmesen, C. 2008. The influence of temperature on the development of Baltic Sea sprat (*Sprattus sprattus*) eggs and yolk sac larvae. Mar. Biol. (Berl.), **154**(2): 295–306. doi:10.1007/s00227-008-0923-1.

Rudstam, L.G., Aneer, G., and Hildén, M. 1994. Top-down control in the pelagic Baltic ecosystem. Dana, **10**: 105–129.

Secor, D.H., and Dean, J.M. 1992. Comparison of otolith-based back-calculation methods to determine individual growth histories of larval striped bass, *Morone saxatilis*. Can. J. Fish. Aquat. Sci. **49**(7): 1439–1454. doi:10.1139/f92-159.

Sirois, P., Lecomte, F., and Dodson, J.J. 1998. An otolith-based back-calculation method to account for time-varying growth rate in rainbow smelt (*Osmerus mordax*) larvae. Can. J. Fish. Aquat. Sci. **55**(12): 2662–2671. doi:10.1139/f98-170.

Sogard, S.M. 1997. Size-selective mortality in the juvenile stage of teleost fishes: a review. Bull. Mar. Sci. **60**(3): 1129–1157.

Takahashi, M., Nishida, H., Yatsu, A., and Watanabe, Y. 2008. Year-class strength and growth rates after metamorphosis of Japanese sardine (*Sardinops melanostictus*) in the western North Pacific Ocean during 1996–2003. Can. J. Fish. Aquat. Sci. **65**(7): 1425–1434. doi:10.1139/F08-063.

Temming, A. 1995. Die quantitative Bestimmung der Konsumtion von Fischen. Experimentelle, methodische und theoretische Aspekte. Habilitation treatise, Fakultät für Mathematik und Naturwissenschaften, University of Hamburg, Hamburg, Germany.

Vigliola, L., and Meekan, M. 2009. The back-calculation of fish growth from otoliths. *In* Tropical fish otoliths: information for assessment, management and ecology. *Edited by* B.S. Green, B.D. Mapstone, G. Carlos, and G.A. Begg. Springer, Heidelberg, Germany. pp. 174–211.

Vigliola, L., Harmelin-Vivien, M., and Meekan, M.G. 2000. Comparison of techniques of back-calculation of growth and settlement marks from the otoliths of three species of *Diplodus* from the Mediterranean Sea. Can. J. Fish. Aquat. Sci. **57**(6): 1291–1299. doi:10.1139/f00-055.

Ware, D.M. 1975. Relation between egg size, growth, and natural mortality of larval fish. J. Fish. Res. Board Can. **32**(12): 2503–2512. doi:10.1139/f75-288.

Wilson, D.T., and McCormick, M.I. 1997. Spatial and temporal validation of settlement-marks in the otoliths of tropical reef fishes. Mar. Ecol. Prog. Ser. **153**: 259–271. doi:10.3354/meps153259.

Wilson, J.A., Vigliola, L., and Meekan, M.G. 2009. The back-calculation of size and growth from otoliths: Validation and comparison of models at an individual level. J. Exp. Mar. Biol. Ecol. **368**(1): 9–21. doi:10.1016/j.jembe.2008.09.005.